

Surface plasmon resonances of optical antenna atomic force microscope tips

Yanshu Zou, Paul Steinvurzel, Tian Yang, and Kenneth B. Crozier^{a)}
 Harvard School of Engineering and Applied Sciences, 33 Oxford Street, Cambridge,
 Massachusetts 02138, USA

(Received 18 December 2008; accepted 6 March 2009; published online 29 April 2009)

A method for fabricating optical antennas on atomic force microscope probes using focused ion beam modification is described. We numerically demonstrate that these optical antenna probes provide a large near field intensity enhancement when illuminated at their resonant wavelengths. We experimentally measure the plasmon resonant wavelengths of probes with various lengths. Both simulation and experiment indicate that the resonant wavelength redshifts with increasing antenna length. We anticipate that the optical antenna tips could be used for mapping the field distributions of nanophotonic devices or for high spatial resolution spectroscopy. © 2009 American Institute of Physics. [DOI: 10.1063/1.3116145]

Scanning near field optical microscopy enables optical imaging on a subwavelength scale below the resolution limit of far field optics.¹ The spatial resolution and signal-to-noise ratio in scattering and tip enhanced optical near field imaging depend on the degree to which the illuminated tip provides a localized spot. This has motivated investigations on how to engineer the tip design for improved near field imaging.^{2,3} Metal nanostructures that efficiently capture or radiate electromagnetic waves at optical frequencies through surface plasmon excitation, so-called optical antennas, are well suited for this problem. In 1985, Wessel⁴ proposed that near field imaging could be performed using a scanned plasmon resonant nanoparticle and drew an analogy to antennas. In 1989, Fischer and Pohl⁵ imaged a metal film by scanning a gold coated polystyrene particle above it. Recent work has focused on more efficient designs, which employ small gaps or very sharp points.^{6–10} There have been several demonstrations of near field optical scanning probes with antenna-type structures, where the antennas are formed by either attaching gold nanoparticles to the tip¹¹ or carving a bow-tie antenna out of a metal film.¹² In both cases, the effective radius of curvature of the antenna tip, which dominates the near field spatial resolution, is much larger than the original radius of curvature for atomic force microscope (AFM) or metal wire tips to which the antenna is attached.

In that vein, we demonstrate a method for fabricating optical antennas on AFM tips that provide a resonant field enhancement while maintaining the original sharpness of the tip. We use silicon nitride (Si_3N_4) tips, which are 3 μm long with a nominal tip radius of 15 nm. We thermally evaporate Au onto the AFM tip to a nominal thickness of 25 nm at 0.6 $\text{\AA}/\text{s}$ [Fig. 1(a)]. We then form the antenna with a focused ion beam (FIB), where we image the tip and mill a square frame around tip end until the antenna reaches the desired length [side view, Fig. 1(b)] and is spatially isolated from the rest of the shaft. The antenna is then a finite conical Au shell with a Si_3N_4 core. We use scanning and transmission electron microscopies (SEM and TEM) [Fig. 1(c)] to estimate the tip radius and length of the optical antennas. The tip radii are measured to be in the range of 15–30 nm, confirming that we

can maintain the sharpness of the original AFM tip during fabrication. This is because the fabrication process here does not involve cutting the end of the tip, unlike bowtie antennas.¹² In the TEM image, it is clear that neither the length of the Au coated region nor the thickness of the Au film are uniform throughout the cross-section of the tip, which add difficulties in quantitative modeling. We define an equivalent tip length by determining the cross-sectional area of the Au coated region from the TEM images. We use this to obtain the length of an equivalent triangle having the same

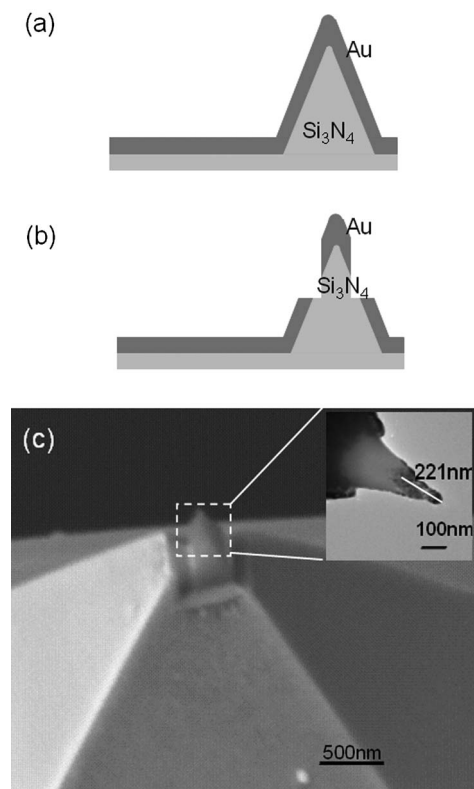


FIG. 1. (a) Diagram of Si_3N_4 AFM tip coated with Au. (b) Diagram of tip after FIB milling. The Au coated tip end, which comprises the optical antenna, is isolated from the rest of the shaft. (c) SEM image of the tip after fabrication. Inset: TEM image of the tip. Dark regions represent Au; lighter regions represent Si_3N_4 .

^{a)}Electronic mail: kcrozier@seas.harvard.edu.

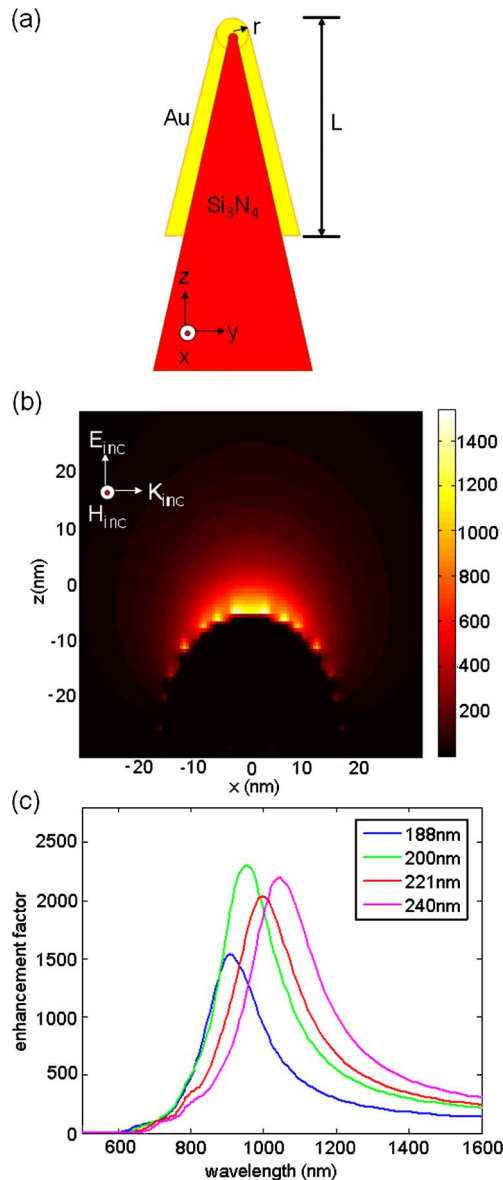


FIG. 2. (Color online) (a) Diagram of simulated optical antenna probe. (b) Field intensity (E^2) distribution for a 188 nm length probe illuminated at the resonance wavelength. (c) Spectral response (E^2 near field enhancement) of antenna probes with varying lengths.

area but with a truncated apex having a width equal to twice the radius of curvature. We successfully fabricated antennas with equivalent lengths varying from 150 to 240 nm.

Previous numerical studies modeled related types of near field probes as infinite cones or as cones with nanostructures at the end of the tip.^{2,3,13,14} Though our AFM tip is pyramidal, the TEM image indicates that the end of the tip is conical, so we use this geometry in our finite difference time domain method simulations for the field enhancement [Fig. 2(a)]. The simulated structure has a tip radius of 15 nm, a cone angle of 30° , and a 20 nm metal coating, where the thickness is estimated from the TEM image. It is slightly thinner than the nominal deposition thickness (25 nm) due to the slower deposition rate on the sloping sides of tips and possible removal of metal during the FIB milling. We vary the length L of the gold coated part between 188 and 240 nm and determine the antenna resonance frequency by simulating the tip scattering response to a quarter cycle optical pulse. The spatial distribution of the excitation is a plane

wave polarized along the axis of the tip (z -direction) and propagating in the $+y$ direction. We use a time monitor placed 1 nm away from the end of the tip to estimate the enhancement factor, defined as the local electric field intensity (E^2) normalized to the local intensity when no tip is present. In Fig. 2(b), simulations of the enhancement factor as a function of wavelength are presented for optical antenna probes with different lengths. For each tip length, we clearly see a strong field enhancement at the antenna resonance wavelength. As expected, the resonance wavelength increases with increasing length. The reason why the peak intensity varies in a nonmonotonic fashion is unknown, though the trend is somewhat akin to what one finds in the simulated spectra of metal nanoshells of different sizes.¹⁵

In Fig. 2(c), we show a representative electric field intensity distribution at the antenna resonance for a 188 nm long tip, where the launch field is a quasi-cw plane wave with a free space wavelength of 892 nm. We obtain an intensity enhancement of ~ 1500 at a distance of 1 nm from the center of the end of the tip. A more realistic estimate of the enhancement factor can be obtained by integrating the field over a 10×10 nm² square area in the xy plane; in this case, the average intensity enhancement factor is ~ 1200 .

We apply dark-field scattering to measure the resonance wavelengths of our fabricated optical antenna probes. Dark-field scattering has previously been used to determine the optical properties of nanoparticles attached to optical fiber probes and of sharp metal tips.^{16,17} The AFM stage is mounted on an inverted optical microscope with a 1.4 numerical aperture (NA) oil-immersion microscope objective lens and a homemade mask to achieve total internal reflection at the surface of a glass coverslip [Fig. 3(a)]. The light source is a tungsten filament lamp. A polarizer is used to ensure that the illumination is p -polarized. This configuration ensures that the tip probes only an evanescent field polarized along the tip axis with a decay length of the order of a few hundred nanometers, thereby suppressing background scattering from other parts of the tip. Measurements are carried out with the tip in contact with the coverslip. The scattered light is collected by a multimode lensed optical fiber and delivered to a charge coupled display (CCD) based spectrometer with a wavelength resolution of 0.5 nm. In order to normalize the scattering spectrum, we divide the scattering spectrum of each tip by a reference spectrum taken without the mask in place and with the antenna probe tip retracted from the coverslip. This corrects for the lamp spectrum and the transmission spectrum of the microscope optics, which are not spectrally flat.

Measured scattering spectra are shown as Fig. 3(b). The spectra are vertically offset for clarity and are obtained for tips with lengths varying from 188 to 240 nm. The resonance wavelength redshifts with the increasing tip length, consistent with the predictions of simulations.

From Fig. 3(c), we find that the resonance wavelengths we measured do not shift with tip length as much as the simulations predict. This is also true of far field simulations (dotted line). There are three possible reasons for this phenomenon. First, we expect a thickness difference caused by FIB milling to cause a shift in resonance wavelength. To understand the effects of nonuniform film thicknesses, we carry out additional simulations of antennas with gold coating thicknesses of 22 and 26 nm. We find that a thicker

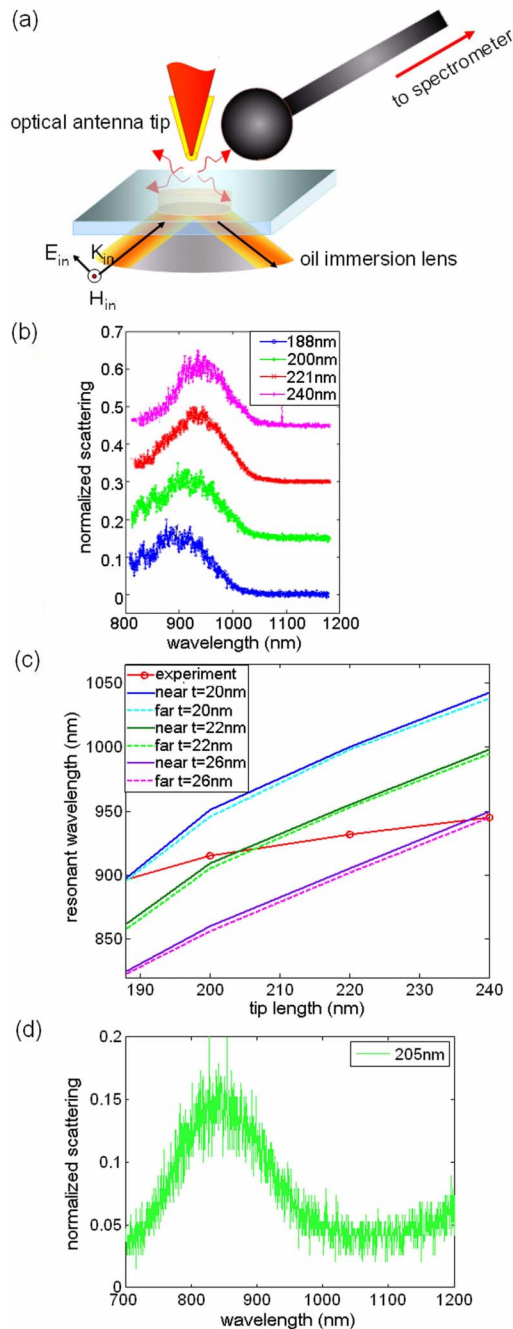


FIG. 3. (Color online) (a) Schematic diagram of the experiment. (b) Scattering spectra of tips with different lengths. (c) Comparison between experimental and simulated (including near field and far field responses with various coating thicknesses t) values of resonance wavelength for varying tip lengths. (d) Scattering spectrum of a 205 nm long Ag tip.

coating leads to a blueshift in resonance wavelength. Second, as discussed earlier, the distance from the end of the tip to the metal edge is not uniform, unlike the simulated structure [Fig. 2(a)]. Third, the tip is illuminated with a plane wave in the simulation, while it is illuminated with the evanescent wave in the experiment. Other possibilities such as the presence of high refractive index glass substrate, which shifts the

resonance with respect to vacuum, might also cause the difference between simulation and experiment.

In tip enhanced fluorescence or Raman scattering, green or red excitation wavelengths are often preferred. This motivates us to blueshift our resonance by using Ag, which has a higher plasma frequency than Au. We measured the resonance wavelength of a fabricated 205 nm Ag tip to be around ~ 840 nm, which corresponds to a blueshift of ~ 60 nm as compared to an Au antenna tip of similar length [see Fig. 3(d)].

In conclusion, we have presented fabrication, modeling, and characterization results for optical antennas formed at the ends of AFM tips. By fabricating the probe directly onto an AFM tip using FIB milling, we can maintain a small tip radius of curvature (15–30 nm) and therefore expect that this will result in high spatial resolution. The combination of the lightning rod effect, enabled by the sharp tip, and the antenna resonance due to the finite length of the metal coating allows us to achieve high intensity enhancement at the resonance wavelength. We experimentally measured scattering resonances associated with the antenna resonance and showed that these can be redshifted by lengthening the metal coated region. The fabricated devices could be used for mapping the near field distribution of nanophotonic devices or nanospectroscopy. Future work will focus on experimental imaging with our antenna probes.

This work is supported by the Microsystems Technology Office (MTO) of the Defense Advanced Research Projects Agency (DARPA) and by the National Science Foundation (NSF). Fabrication work was carried out at the Harvard Center for Nanoscale Systems, which is supported by the NSF. The authors thank Nanfang Yu and Eric Kort for fruitful discussions and Richard Schalek for assistance in doing FIB.

- ¹L. Novotny and B. Hecht, *Principles of Nano-Optics* (Cambridge University Press, Cambridge, 2006).
- ²Y. C. Martin, H. F. Hamann, and H. K. Wickramasinghe, *J. Appl. Phys.* **89**, 5774 (2001).
- ³J. T. Krug, E. J. Sanchez, and X. S. Xie, *J. Chem. Phys.* **116**, 10895 (2002).
- ⁴J. Wessel, *J. Opt. Soc. Am. B* **2**, 1538 (1985).
- ⁵U. Ch. Fischer and D. W. Pohl, *Phys. Rev. Lett.* **62**, 458 (1989).
- ⁶R. D. Grober, R. J. Schoelkopf, and D. E. Prober, *Appl. Phys. Lett.* **70**, 1354 (1997).
- ⁷K. B. Crozier, A. Sundaramurthy, G. S. Kino, and C. F. Quate, *J. Appl. Phys.* **94**, 4632 (2003).
- ⁸P. Mühlischlegel, H.-J. Eisler, O. J. F. Martin, B. Hecht, and D. W. Pohl, *Science* **308**, 1607 (2005).
- ⁹L. Novotny, *Phys. Rev. Lett.* **98**, 266802 (2007).
- ¹⁰A. Alu and N. Engheta, *Phys. Rev. Lett.* **101**, 043901 (2008).
- ¹¹S. Kühn, U. Hakanson, L. Rogobete, and V. Sandoghdar, *Phys. Rev. Lett.* **97**, 017402 (2006).
- ¹²J. N. Farahani, H. J. Eisler, D. W. Pohl, M. Pavius, P. Flückiger, P. Gasser, and B. Hecht, *Nanotechnology* **18**, 125506 (2007).
- ¹³R. M. Roth, N. C. Paniou, M. M. Adams, R. M. Osgood, C. C. Neacsu, and M. B. Raschke, *Opt. Express* **14**, 2921 (2006).
- ¹⁴L. Novotny, R. X. Bian, and X. S. Xie, *Phys. Rev. Lett.* **79**, 645 (1997).
- ¹⁵N. Halas, *Opt. Photonics News* **Aug**, 26 (2002).
- ¹⁶S. K. Eah, H. M. Jaeger, N. F. Scherer, G. P. Wiederrecht, and X. M. Lin, *Appl. Phys. Lett.* **86**, 031902 (2005).
- ¹⁷C. C. Neacsu, G. A. Steudle, and M. B. Raschke, *Appl. Phys. B: Lasers Opt.* **80**, 295 (2005).